

# SOA-based interferometric optical hard-limiter

G. T. Kanellos, N. Pleros, C. Bintjas, H. Avramopoulos

National Technical University of Athens – Department of Electrical Engineering and Computer Science  
9 Iroon Polytechniou Street, Zografou 15773 –Athens, Greece  
Tel. +30-10-772 2057, Fax +30-10-7722077, Email: gkanel@cc.ece.ntua.gr

and G. Guekos

Swiss Federal Institute of Technology Zurich, ETH Hoenggerberg, CH-8093 Zurich, Switzerland

**Abstract:** We present experimental and theoretical analysis of an optical hard limiter that uses SOA-based interferometers. Its operation relies on the deep saturation of SOA and it can suppress amplitude modulation in excess of 10 dB.

©2004 Optical Society of America

**OCIS codes:** (250.4480) Optical amplifiers; (070.4560) Optical data processing;

## 1. Introduction

Semiconductor Optical Amplifier (SOA)-based all-optical gates have been used extensively in recent years to demonstrate a number of network functionalities [1], due to their capability for high speed, bit-wise processing and their potential for integration. The high speed capability of the SOA-based gates is due to the relatively short carrier recovery time and high gain of SOAs, but besides speed, these two properties can also be exploited to effect high speed optical signal conditioning [2]. In this respect we have recently demonstrated an optical clock recovery circuit which is capable for operation with short, asynchronous optical packets and which relies on the saturation properties of a SOA-based optical gate for its operation [3].

In the present article we demonstrate that an SOA-based gate can be used as an optical hard limiter circuit, when saturated by a strong CW signal. We experimentally demonstrate the hard-limiting power transfer function of an Ultra-fast Nonlinear Interferometer (UNI) at 10 GHz and develop a theoretical transfer function analysis to verify the experimental results. The increased power equalization properties of the gate is achieved by clamping the output power to a constant level for input power levels greater than a specific threshold, when the SOA gain is appropriately biased. Experimental and theoretical analysis show good agreement and reveal input pulse power fluctuation suppression in excess of 10 dB.

## 2. Experiment

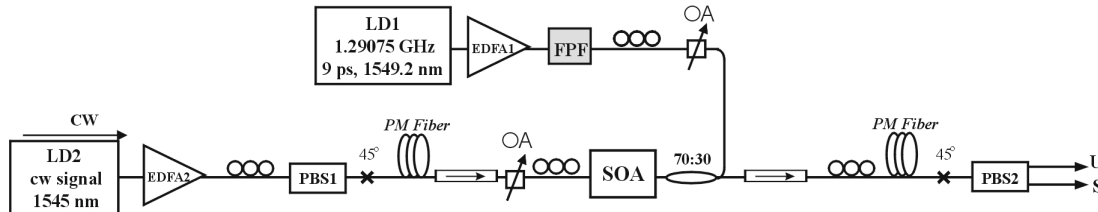


Fig. 1. Experimental setup. FPF: Fabry-Perot filter, OA: optical attenuator, PC: Polarization Controller, PBS: Polarization Beam Splitter, PM Fiber: Polarization Maintaining Fiber

Fig. 1 shows the experimental setup of the hard-limiter, comprising a UNI gate that is powered by a CW signal, provided by a DFB laser diode at 1545 nm (LD2) and which determines the saturation level of the SOA. The interferometric switch used is a UNI gate optimized for operation at 10.326 Gb/s. The active element is a 1.5 mm bulk SOA with 30 dB peak small signal gain at 1560 nm and 80 ps recovery time, when driven with 700 mA dc current. The  $U_{\text{sat}}$  parameter of the amplifier was found to be approximately 10 fJ.

In order to demonstrate the power equalizing properties of the gate and extract the power transfer function of the saturated SOA-based interferometer, we have used a control signal with controllable amplitude modulation. A DFB laser diode (LD1) at 1549.2 nm, gain switched at 1.29075 GHz, provides a clock stream of 8 ps pulses. This clock signal enters into a Fabry-Perot filter with low finesse of 20.7 and Free Spectral Range (FSR) at 10.326 GHz. The exponentially decaying impulse response of the filter provides a clock signal at 10.326 GHz that exhibits a periodic amplitude modulation of 8 bits period and a maximum value of approximately 9 dB, as shown in Fig. 2(a).

Fig. 2(b), 2(c) and 2(d) illustrate the corresponding switched signal for three indicative control signal powers inserted into the SOA, namely 200  $\mu\text{W}$ , 600  $\mu\text{W}$  and 800  $\mu\text{W}$ , respectively. The amplitude modulation imposed on the switched pulses reduces to 7, 2.4 and 0.8 dB, respectively, as the control signal power increases. The CW power

level that is used for deep saturation of the SOA, is 1 mW. Using the same CW power level, this measurement procedure was repeated for different control signal power values inserted into the SOA in order to cover a broad range of control pulse energies. The black circles in fig. 3(b) indicate the experimental results for the transfer function of the normalized output vs input, after correlating the switched output pulse energy to the respective control pulse energy for every injected control signal average power level. These results show that beyond a certain input pulse energy threshold, the output power is clamped to a constant level irrespective of the inserted control pulse energy. In this way, the switched power curve takes a strongly non-linear step-like form that is almost parallel to the x-axis and clearly possesses the characteristics of a hard limiter.

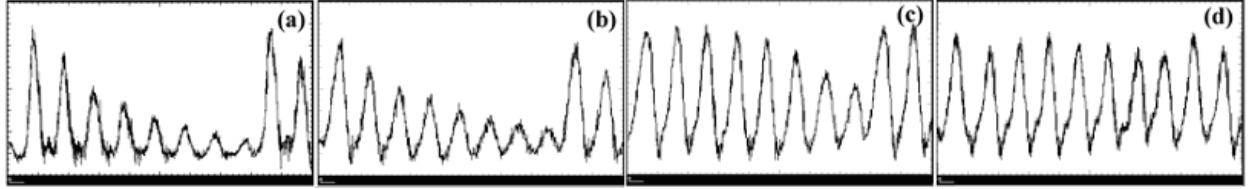


Fig. 2. Oscilloscope traces of : (a) Incoming control signal, indicating the period of 8 bits and the controllable amplitude modulation. (b), (c), (d): switched output signal for different average powers Of 200  $\mu$ W, 600  $\mu$ W and 800  $\mu$ W respectively.

## 2. Theoretical Analysis

The hard-limiting properties of a device are expressed by its ability to provide power amplitude equalization. To relate the input and output amplitude modulation indexes  $m$  and  $m_{o/p}$  respectively, we define the amplitude modulation reduction (AMR) index as  $AMR=10 \cdot \log|m_{o/p}/m|$ . We develop a theory to obtain an analytical expression of the AMR for SOA-based interferometric devices with saturated SOAs, proving their operation as hard limiters and exploring their performance limitations.

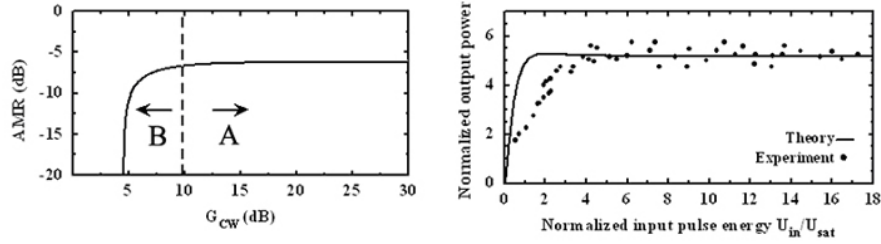


Fig. 3. (a): Amplitude modulation reduction (AMR) vs the steady-state gain value  $G_{CW}$  of the SOA that describes its saturation level (b): experimental and theoretical power transfer function.

We consider a MZI switch with a SOA in each of its arms [4] and we assume that the SOAs are identical devices. The MZI is powered by a CW signal whereas a pulsed optical beam is used as the control signal responsible for the non-linear response in one of the SOAs. The switched part of the CW signal at the output is given by [3]

$$P_s(t) = \frac{P_{CW}}{4} \left[ G_1(t) + G_{CW} - 2\sqrt{G_1(t)G_{CW}} \cdot \cos(\Delta\phi(t)) \right] \quad (1)$$

where  $P_{CW}$  is the CW signal input optical power,  $G_1(t)$  and  $G_{CW}$  are the upper and lower branch SOA gains, respectively, and  $\Delta\phi(t)$  is the phase difference between the two CW components, induced by the control signal, provided by [5]

$$\Delta\phi(t) = -\frac{\alpha}{2} \ln[G_1(t)/G_{CW}] \quad (2)$$

with  $\alpha$  denoting the linewidth enhancement factor of each SOA.

The  $G_{CW}$  gain is the time-independent equilibrium gain since no control pulse is inserted into the lower branch SOA. The  $G_{CW}$  value is determined only by the SOA small-signal gain  $G_0$  and the  $P_{CW}$  input power [6]. On the other hand, in the case of single control pulse insertion,  $G_1(t)$  is provided by [6]

$$G_1(t) = \left[ 1 - \left( 1 - (1/G_{CW}) \right) \exp(-U_{in}(t)/U_{sat}) \right]^{-1} \quad (3)$$

where  $U_{in}(t)$  is the accumulated injected control pulse energy and  $U_{sat}$  is the saturation energy of the SOA. After the whole pulse energy has passed through the SOA, the gain recovers back to its initial  $G_{CW}$  value with the stimulated carrier lifetime constant [7].

We assume an amplitude modulated control pulse stream where the energy of the  $k$ -th individual control pulse is expressed as  $U_{in}^k(t) = P_0(1 + m \cdot \cos(\Omega \cdot k \cdot T)) \cdot A$ .  $P_0$  is the average peak power value,  $m$  is the modulation depth

index,  $\Omega$  is the modulation frequency,  $T$  is the bit period and  $A$  is a constant that emerges from the pulse shape. Using the gain (3) and phase (2) equations into (1) and by satisfying the requirement for an average  $\pi$  phase shift, we solve with respect to the output modulation index  $m_{o/p}$ :

$$m_{o/p} = \frac{\left(1 + \exp\left(\frac{\pi}{\alpha}\right)\right) \cdot \exp\left(-\frac{2\pi}{\alpha}\right) \cdot \left(1 - G_{CW} \cdot \exp\left(-\frac{2\pi}{\alpha}\right)\right)}{1 + \exp\left(-\frac{2\pi}{\alpha}\right) + 2 \cdot \exp\left(-\frac{\pi}{\alpha}\right)} \cdot \ln\left(\frac{1 - \frac{1}{G_{CW}}}{1 - \frac{1}{G_{CW}} \cdot \exp\left(\frac{2\pi}{\alpha}\right)}\right) \cdot m \quad (4)$$

Eq. (4) provides the transfer function characteristics of the gate for every amplitude modulating signal frequency component. It shows that the output amplitude modulation index  $m_{o/p}$  depends only on the gain  $G_{CW}$  and the  $\alpha$ -parameter of the SOA while it is linearly related to the input modulation index.

Fig. 3(a) provides a plot of the AMR index in log scale for different  $G_{CW}$  values, using Eq. (4). When the SOA operates in the unsaturated regime, that corresponds to gain values between 10 and 30 dB, the gate exhibits a constant amplitude modulation reduction of approximately 6 dB. By increasing the CW power, the SOA is heavily saturated and the gate operates as a hard limiter, reducing the input amplitude modulation in excess of 10 dB. The power equalization properties are exhausted when the SOA operates close to transparency, at a limit of  $10 \cdot \log[\exp(2\pi/\alpha)]$  that is dictated by the requirement for  $\pi$  phase shift. At this point, the amplitude modulation reduction can exceed 30dB, at the cost of using increased CW power.

The transfer function of the unsaturated gate has the well-known near sinusoidal form that is responsible for the 6 dB amplitude modulation reduction. However, when the SOA is saturated and the value of  $G_{CW}$  lies within the range indicated by region B in Fig. 3(a), the switched power curve transforms to an almost step function. The solid line in Fig. 3(b) shows the theoretically obtained transfer function of the gate for a linear  $G_{CW}$  close to the gain limit. Comparison between the theoretical curve and the experimental results in Fig. 3(b) shows good agreement and confirms the successful demonstration of the optical hard-limiting properties of saturated optical gates. Minor variations between the two curves, especially for small values of the input power, are presumably due to the non-negligible internal losses of the SOA.

It should be noted that the use of different interferometric structures for the experimental and theoretical analysis, respectively, does not impair the conclusions of this study or the validity of the agreement. For the hard-limiting operation, the key parameter is only the degree of saturation of the SOA, rather than the specific architecture of the interferometer. The SOA is biased by the CW signal close to its material transparency but in a way that a  $\pi$  phase shift can be still obtained when a control pulse with appropriate energy level is injected. As such, the output power increases with the control pulse energy until a  $\pi$  phase shift is obtained, but then greater control pulse energies cause again an almost  $\pi$  phase shift, since the SOA operates now at transparency and its gain has reached its unitary end-point. As a result, the saturated optical gate acts as an optical hard-limiter, verifying its potential to provide increased input pulse power fluctuation suppression in excess of 10 dB.

#### 4. Conclusion

In conclusion, we have presented both theoretically and experimentally the successful operation of a deeply saturated SOA-based interferometric gate as an optical hard-limiter. This circuit reveals the ability of SOA-based gates to effect to optical signal conditioning. This fact is important not only because it can lead to novel functional subsystems for optical packet switching applications [1] but mainly because it can be used to offer enhanced performance characteristics to optical signal processing [8] and Optical Code-Division Multiple-Access (OCDMA) systems [9].

#### References

- [1] C. Bintjas, K. Vlachos, N. Pleros and H. Avramopoulos, "Ultrafast Nonlinear Interferometer (UNI)-based digital optical circuits and their use in packet switching", *J. Lightwave Technol.* **21**, 2629 (2003)
- [2] L. Brzozowski and E. H. Sargent, "All-optical analog-to-digital converters, hardlimiters, and logic gates", *J. Lightwave Technol.* **19**, 114 (2001)
- [3] N. Pleros et al., "All-optical clock recovery from asynchronous data packets at 10 Gb/s" *IEEE Photon. Technol. Lett.* **15**, 1291-1293 (2003)
- [4] L. Xu, B. C. Wang, V. Baby, I. Glesk, and P. R. Prucnal, "All-optical data format conversion between RZ and NRZ based on a Mach-Zehnder Interferometric wavelength converter", *IEEE Photon. Technol. Lett.* **15**, 308 (2003).
- [5] M. Eiselt, W. Pieper and H. G. Weber, "SLALOM: Semiconductor laser amplifier in a loop mirror", *J. Lightwave Technol.* **13**, 2099 (1995)
- [6] G. P. Agrawal and N. A. Olsson, "Self-Phase Modulation and spectral broadening of optical pulses in semiconductor laser amplifiers", *IEEE J. Quantum Electron.* **25**, 2297 (1989)
- [7] R. J. Manning and D. A. O. Davies, "Three-wavelength device for all-optical signal processing", *Opt. Lett.* **19**, 889 (1994)
- [8] N. Pleros, C. Bintjas, G. T. Kanellos, K. Vlachos, H. Avramopoulos and G. Guekos, "Recipe for amplitude modulation reduction in SOA-based interferometric switches", submitted to *J. Lightwave Technol.*
- [9] J.-J. Chen and G.-C. Yang, "CDMA fiber-optic systems with optical hard limiters", *J. Lightwave Technol.* **19**, 950 (2001)